Inorganic Chemistry

Article

pubs.acs.org/IC

# Novel Barium–Organic Incorporated Iodometalates: Do They Have Template Properties for Constructing Rare Heterotrimetallic Hybrids?

Shashank Mishra,*[,†] Erwann Jeanneau,[‡] Gilles Ledoux,[§] and Stéphane Daniele*[,†]

[†]Université Lyon 1, IRCELYON, CNRS-UMR 5256, 2 Avenue A. Einstein, 69626 Villeurbanne, France

[‡]Université Lyon 1, Centre de Diffractométrie Henri Longchambon, 5 rue de La Doua, 69100 Villeurbanne, France

[§]Université Lyon 1, Institut Lumière Matière, UMR 5306 CNRS, Bâtiment Kastler, 10 rue Ada Byron, 69622 Villeurbanne, France

Supporting Information

**ABSTRACT:** New barium–organic derivatives are introduced as countercations in the iodocuprates and -argentates to yield novel hybrids with unique structural motifs and bonding modes, many of them also showing vivid fluorescence on exposure to UV light. The tetrahedral $MX_4$/trigonal-coplanar $MX_3$ unit in these hybrids $[Ba_2(DMSO)_{12}Cu_8I_{12}]$ (**1**) and $[Ba(tetraglyme)_2]_2[Ag_8I_{12}]\cdot EtOH$ (**7**) can be replaced by the $M'I_4/M'I_3$ unit without compromising their basic structural motifs, thus leading to the formation of the rare mixed Cu–Ag iodometalates $[Ba_2(DMSO)_{12}Cu_4Ag_4I_{12}]$ (**9**) and $[Ba(tetraglyme)_2]_2[CuAg_7I_{12}]\cdot EtOH$ (**10**), respectively. In contrast, a breakdown in the structure-directing properties of these iodometalates was observed in the mixed Ag–Pb iodometalate $[Ba(tetraglyme)_2]_2[Pb_2Ag_2I_{10}]\cdot 2Me_2CO$ (**11**), where the basic structure of the synthon $[Ba(tetraglyme)_2]_2[Ag_4I_8]$ (**8**) was not retained due to the compulsory molecular rearrangement required as a result of replacing $AgI_4/AgI_3$ units with octahedral $PbI_6$ units.

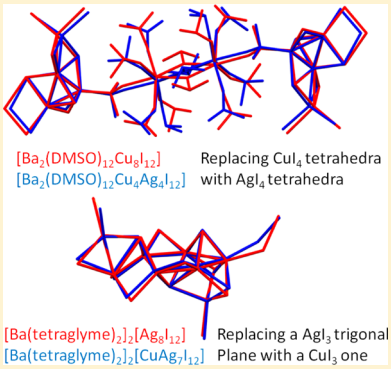


## INTRODUCTION

The family of inorganic–organic hybrid compounds containing metal halides opens a versatile access to innovative advanced materials, owing to their great variety of intriguing structural topologies, fascinating properties (semiconducting/insulating, excitonic, thermochromism, third-order nonlinear optics, ferroelectrics, ...), and potential technological applications in many fields such as ionic liquids, optics, magnetism, photovotaics, and sensing.[1] Among these, those containing copper(I) and silver(I) halide moieties have received special attention for their structural diversity, luminescent uniqueness,[2] and ability to form metal–organic frameworks,[3] where the metallophilic M(I)···M(I) (M = Cu, Ag) interaction helps to sustain porous structures. The properties of these hybrids can further be tuned by introducing an additional metal to it. One strategy to do so is to employ a metal–organic cation, instead of the commonly used organic cation.[4,5] Alternatively, the additional metal can also be brought by the anionic moiety to yield heterometallic halometalates.[6,7] These two strategies usually yield hybrids with different properties as, unlike intimate interaction often observed between two metals in the heterometallic halometalates, the metal–organic cation in the former case mostly acts as a discrete countercation without having a significant interaction with the halometalate part. Both strategies have been employed in the case of halometalate hybrids of group 11, and quite a few examples are available in both cases: i.e., halocuprates and -argentates having a metal–organic cation (primarily comprised of transition metals and lanthanides)[5] and heterometallic halocuprates and -argentates (mostly with Pb and Bi).[7] In principle, it is possible to combine these two strategies and thus to introduce two additional metals which would bring new properties to these hybrid materials by the synergic effects of three metals. However, heterotrimetallic halometalates are very rare and, to date, only a handful of such hybrids are known.[8] Moreover, there is absolutely no report available on their systematic synthesis and structural design. Here we introduce barium–organic cations to generate novel iodocuprates and -argentates with interesting structural motifs and topologies. The basic idea was to see whether these hybrid iodometalates can serve, in general, as templates for constructing unique metal–organic incorporated heterometallic iodometalates containing three different metals. We herein show that the above iodometalates can not only be used as synthons but also have structure-directing effects. As a general trend, the basic structure of metal–organic-containing halometalates is retained when a tetrahedral $MI_4$ or a trigonal-coplanar $MI_3$ unit is replaced by another $M'I_4$/ $M'I_3$ unit. In contrast, replacing a $MI_4/MI_3$ unit with an octahedral $M'I_6$ unit leads to a breakdown in the structure-directing properties of these iodometalates due to the compulsory molecular rearrangement required.

**Received:** August 12, 2014
**Published:** October 22, 2014

   dx.doi.org/10.1021/ic501963y | *Inorg. Chem.* 2014, 53, 11721–11731

## EXPERIMENTAL SECTION

**General Procedures.** All manipulations were carried out under argon using Schlenk tubes and vacuum line techniques. $BaI_2$, $BaI_2 \cdot 2H_2O$, CuI, AgI, $PbI_2$, $NH_4I$, DMSO, and glymes (all Aldrich) were used as received. Solvents were purified on an MB SPS-800 instrument. FT-IR spectra were recorded as KBr pallets on a Bruker Vector 22 spectrometer. Melting points were measured on a Reichert (Austria) instrument and were uncorrected. Analytical data were obtained from the Service Central d'Analyses du CNRS. The diffuse reflectance spectra of the crystalline samples were recorded at room temperature from 200 to 700 nm on a PerkinElmer Lamda 35 spectrophotometer. Powder X-ray diffraction data were obtained with a Siemens D 5000 diffractometer using Cu K$\alpha$ radiation. Luminescence spectra of the crystalline samples were recorded at room temperature on a homemade spectrometer using the laser-driven light source (LDLS) eq 99 from Energetiq as the excitation source. The excitation was filtered by a Gemini 180 JobinYvon monochromator with 2 mm slits ensuring an excitation resolution of 4 nm. The luminescence was collected by an optical fiber coupled with a TRIAX320 Jobin Yvon monochromator. The light was then detected by a Peltier cooled CCD camera. The resolution used in emission was 1.5 nm.

**Synthesis of 1−11.** *$[Ba_2(DMSO)_{12}Cu_8I_{12}]$ (**1**).* A DMSO solution of $NH_4I$ (2 mL, 4 M) was added dropwise to a suspension of CuI (1.79 g, 9.40 mmol) in 3 mL of DMSO, and the obtained clear yellow solution was transferred to a prestirred suspension of $BaI_2$ (0.94 g, 2.41 mmol) in 2 mL of DMSO. After the mixture was stirred for 3 h at room temperature, the clear solution obtained was layered with 7 mL of ethanol. Colorless blocks of **1** grew overnight, which were separated after decantation of the DMSO/ethanol layers. Yield: 3.27 g (84% wrt $BaI_2$). Mp: 105 °C. Anal. Found: C, 8.82; H, 2.18; Ba, 8.41; Cu, 15.72. Calcd for $C_{24}H_{72}Ba_2O_{12}S_{12}Cu_8I_{12}$ (3243.5): C, 8.88; H, 2.22; Ba, 8.46; Cu, 15.67. FT-IR (KBr, $cm^{-1}$): 1622w, 1432s, 1408s, 1312s, 1028s, 947s, 897w, 707m, 674w, 480w.

By adoption of a procedure similar to that described for **1**, complexes **1a**, **2**, and **3** were also synthesized using the appropriate quantities (given in parentheses) of $BaI_2$ (or $BaI_2 \cdot 2H_2O$), CuI/AgI, and a 4 M solution of $NH_4I$ in DMSO and crystallized by layering the DMSO solution with ethanol.

*$[Ba_2(DMSO)_{12}(H_2O)_2Cu_8I_{12}]$ (**1a**).* $BaI_2 \cdot 2H_2O$ (0.79 g, 1.84 mmol) and CuI (1.39 g, 7.30 mmol) in 7 mL of DMSO, $NH_4I$ (2 mL, 4 M). Yield: 5.40 g (89%). Mp: 95 °C. Anal. Found: C, 8.83; H, 2.35; Ba, 8.45; Cu, 15.57. Calcd for $C_{24}H_{76}Ba_2O_{14}S_{12}Cu_8I_{12}$ (3279.56): C, 8.78; H, 2.32; Ba, 8.37; Cu, 15.50. FT-IR (KBr, $cm^{-1}$): 3400br, 1632w, 1434m, 1411m, 1312s, 1030s, 954s, 897w, 710m, 698w.

*$[Ba_2(DMSO)_{13}]_2[Ag_{14}I_{22}]$ (**2**).* $BaI_2$ (0.51 g, 1.31 mmol) and AgI (1.14 g, 4.85 mmol) in 7 mL of DMSO, $NH_4I$ (2 mL, 4 M). Yield: 1.77 g (79% with respect to $BaI_2$). Mp: 120 °C. Anal. Found: C, 8.94; H, 2.25; Ag, 21.90; Ba, 7.93. Calcd for $C_{52}H_{156}Ba_4O_{26}S_{26}Ag_{14}I_{22}$ (6882.9): C, 9.06; H, 2.27; Ag, 21.94; Ba, 7.97. FT-IR (KBr, $cm^{-1}$): 1609w, 1560w, 1431m, 1400s, 1311m, 1303w, 1261w, 1031s, 954s, 933m, 897w, 821w, 800w, 704m, 671w.

*$[Ba_2(DMSO)_{12}(H_2O)](H_3O)[Ag_6I_{11}] \cdot 2DMSO$ (**3**).* $BaI_2 \cdot 2H_2O$ (0.73 g, 1.70 mmol) and AgI (1.21 g, 5.15 mmol) in 8 mL of DMSO, $NH_4I$ (2 mL, 4 M). Yield: 2.17 g (74%). Mp: 100 °C. Anal. Found: C, 9.79; H, 2.60; Ag, 18.85; Ba, 8.01. Calcd for $C_{24}H_{74}Ba_2O_{13}S_{12}Ag_6I_{11} \cdot 2C_2H_6OS \cdot H_3O$ (3448.7): C, 9.74; H, 2.58; Ag, 18.76; Ba, 7.96. FT-IR (KBr, $cm^{-1}$): 3440br, 1636m, 1435s, 1410s, 1312m, 1291w, 1025s, 954s, 897w, 706m, 673w $cm^{-1}$.

*$[Ba(tetraglyme)_2][Cu_2I_4]$ (**4**).* An acetone solution of CuI (0.43 g, 2.27 mmol) and $NH_4I$ (2 mL, 4 M) in acetone (10 mL) was added to a suspension of $BaI_2 \cdot 2H_2O$ (0.33 g, 0.77 mmol) and tetraglyme (1.5 mL) in acetone (10 mL), and the resulting reaction mixture was stirred for 4 h. Removal of solvents under vacuum afforded a pale yellow solid. Yield: 0.93 g (99% with respect to $BaI_2 \cdot 2H_2O$). Mp: 230 °C dec. A part of this solid (0.5 g) was recrystallized from acetone (40 mL) at 0 °C. Anal. Found: C, 19.79; H, 3.65; Ba, 11.19; Cu, 10.40. Calcd for $C_{20}H_{44}BaO_{10}Cu_2I_4$ (1216.61): C, 19.72; H, 3.62; Ba, 11.28; Cu, 10.45. FT-IR (KBr, $cm^{-1}$): 2987w, 2923m, 2878m, 2833m, 2368w, 2355w, 1447m, 1345m, 1286m, 1242m, 1195m, 1090s, 1055s, 1016s, 982w, 943s, 865m, 849s, 823m, 530w, 457w.

The complexes **5**−**8** were prepared using a similar procedure and crystallized from either acetone alone or an acetone/ethanol combination.

*$[Ba(triglyme)_2(acetone)_2][Cu_4I_6]$ (**5**).* $BaI_2 \cdot 2H_2O$ (0.42 g, 0.98 mmol), triglyme (1 mL), CuI (0.78 g, 4.09 mmol), $NH_4I$ (2 mL, 4 M) in acetone (15 mL). Yield: 1.45 g (91%). Mp: 122 °C. Anal. Found: C, 16.20; H, 2.91; Ba, 8.40; Cu, 15.67. Calcd for $C_{22}H_{48}BaO_{10}Cu_4I_6$ (1625.57): C, 16.24; H, 2.95; Ba, 8.45; Cu, 15.64. FT-IR (KBr, $cm^{-1}$): 2990w, 2922m, 2870m, 2826m, 2366w, 2355w, 1606m, 1455m, 1346m, 1294m, 1245m, 1196m, 1087s, 1058s, 1010m, 984w, 932m, 859m, 837m, 667w, 618w, 532w, 456w, 420w.

*$[Ba(diglyme)_3(H_2O)][Cu_4I_6]$ (**6**).* $BaI_2 \cdot 2H_2O$ (0.5 g, 1.17 mmol), diglyme (1 mL), CuI (0.82 g, 4.30 mmol), $NH_4I$ (2 mL, 4 M) in acetone (45 mL). Yield: 1.56 g (85%). Mp: 315 °C dec. Anal. Found: C, 13.67; H, 2.74; Ba, 8.80; Cu, 16.20. Calcd for $C_{18}H_{44}BaO_{10}Cu_4I_6$ (1573.46): C, 13.73; H, 2.80; Ba, 8.72; Cu, 16.15. FT-IR (KBr, $cm^{-1}$): 3473br, 3387br, 3144br, 2995w, 2922m, 2876m, 2829m, 2364w, 2341w, 1624m, 1452m, 1396m, 1349m, 1285m, 1243m, 1212m, 1121m, 1099s, 1058s, 1001m, 940m, 862s, 826m, 668w, 563w, 459w, 418w.

*$[Ba(tetraglyme)_2]_2[Ag_8I_{12}] \cdot EtOH$ (**7**).* $BaI_2 \cdot 2H_2O$ (0.46 g, 1.07 mmol), tetraglyme (1 mL), AgI (1.02 g, 4.34 mmol), and $NH_4I$ (2 mL, 4 M) in acetone (25 mL), followed by crystallization by carefully layering the acetone solution with ethanol (10 mL). Yield: 3.13 g (81%). Mp: deliquescent. Anal. Found: C, 13.91; H, 2.57; Ag, 24.08; Ba, 7.70. Calcd for $C_{42}H_{94}Ag_8Ba_2I_{12}O_{21}$ (3595.6): C, 14.02; H, 2.61; Ag, 24.00; Ba, 7.64. FT-IR (KBr, $cm^{-1}$): 3340br, 2990w, 2923m, 2881m, 2822m, 2365w, 2348w, 1450m, 1357m, 1339m, 1290m, 1241m, 1196m, 1095s, 1075s, 1054s, 1016s, 977w, 940s, 867m, 840m, 821m, 523w.

*$[Ba(tetraglyme)_2]_2[Ag_4I_8]$ (**8**).* $BaI_2 \cdot 2H_2O$ (0.40 g, 0.94 mmol), tetraglyme (1 mL), AgI (0.48 g, 2.04 mmol), $NH_4I$ (2 mL, 4 M) in acetone (20 mL), followed by crystallization by carefully layering the acetone solution with toluene (10 mL). Yield: 2.27 g (93%). Mp: 180 °C. Anal. Found: C, 18.30; H, 3.40; Ba, 10.58; Ag, 16.60. Calcd for $C_{40}H_{88}Ba_2O_{20}Ag_4I_8$ (2610.5): C, 18.39; H, 3.37; Ba, 10.52; Ag, 16.53. FT-IR (KBr, $cm^{-1}$): 3000w, 2925m, 2884m, 2825m, 2368w, 2348w, 1452m, 1356m, 1342m, 1294m, 1240m, 1196m, 1096s, 1076s, 1056s, 1014s, 982w, 943s, 865m, 845s, 823m, 528w.

*$[Ba_2(DMSO)_{12}Cu_4Ag_4I_{12}]$ (**9**).* The reaction of **1** (1.30 g, 0.40 mmol) with AgI (0.05 g, 0.21 mmol) in the presence of $NH_4I$ (1 mL, 4 M) in DMSO (6 mL), followed by stirring for 8 h and crystallization by carefully layering the concentrated solution with ethanol (4 mL) at room temperature, gave colorless blocks. Yield: 0.86 g (63%). Mp: 100 °C. Anal. Found: C, 8.40; H, 2.12; Ag, 12.59; Ba, 8.10; Cu, 7.50. Calcd for $C_{24}H_{72}Ba_2O_{12}S_{12}Ag_4Cu_4I_{12}$ (3420.80): C, 8.42; H, 2.10; Ag, 12.61; Ba, 8.02; Cu, 7.43. FT-IR (KBr, $cm^{-1}$): 1628w, 1431m, 1414m, 1313m, 1030s, 951s, 918w, 709m, 674w.

*$[Ba(tetraglyme)_2]_2[CuAg_7I_{12}] \cdot EtOH$ (**10**).* The reaction of **7** (1.03 g, 0.29 mmol) with CuI (0.10 g, 0.52 mmol) in the presence of $NH_4I$ (2 mL, 4 M) in acetone (15 mL), followed by stirring for 8 h and crystallization by carefully layering the concentrated solution with ethanol (10 mL) at room temperature, gave colorless needle-shaped crystals. Yield: 0.74 g (74%). Mp: 184 °C. Anal. Found: C, 14.0; H, 2.55; Ag, 21.37; Ba, 7.81; Cu, 1.85. Calcd for $C_{40}H_{88}Ba_2O_2CuAg_7I_{12} \cdot C_2H_6O$ (3551.36): C, 14.20; H, 2.65; Ag, 21.26; Ba, 7.73; Cu, 1.79. FT-IR (KBr, $cm^{-1}$): 3454br, 2925w, 2875w, 2850w, 1698w, 1617m, 1454m, 1404w, 1378w, 1348m, 1294m, 1247m, 1207m, 1093s, 1062s, 1008w, 942w, 943s, 865m, 833s, 727w, 619w, 538w, 462w.

*$[Ba(tetraglyme)_2]_2[Pb_2Ag_2I_{10}] \cdot 2Me_2CO$ (**11**).* The reaction of **8** (1.15 g, 0.44 mmol) with $PbI_2$ (0.13 g, 0.22 mmol) in the presence of $NH_4I$ (2 mL, 4 M) in acetone (75 mL), followed by stirring for 8 h and crystallization from the concentrated solution at 0 °C, gave orange yellow crystals. Yield: 0.74 g (51%). The solvated acetone molecules were removed when the crystals were dried under vacuum. Mp: 225 °C. Anal. Found: C, 15.80; H, 2.95; Ag, 6.98; Ba, 8.90; Pb, 13.65. Calcd for $C_{40}H_{88}Ba_2O_{20}Pb_2Ag_2I_{10}$ (3063.3): C, 15.67; H, 2.87; Ag, 7.04; Ba, 8.96; Pb, 13.53. FT-IR (KBr, $cm^{-1}$): 2930m, 2875w, 2829w,


dx.doi.org/10.1021/ic501963y | Inorg. Chem. 2014, 53, 11721−11731

**Table 1. Crystallographic and Refinement Data of Iodocuprates 1−11**

| | 1 | 1a | 2 | 3 | 4 | 5 |
|---|---|---|---|---|---|---|
| empirical formula | $C_{12}H_{36}BaO_6S_6Cu_4I_6$ | $C_{12}H_{38}BaO_7S_6Cu_4I_6$ | $C_{26}H_{78}Ba_2O_{13}S_{13}\cdot 0.5Ag_{14}I_{22}$ | $C_{24}H_{72}Ba_2O_{13}S_{12}\cdot Ag_6I_{11}\cdot 2C_2H_6OS\cdot H_3O$ | $C_{20}H_{44}BaO_{10}\cdot Cu_2I_4$ | $C_{22}H_{48}BaO_{10}\cdot Cu_4I_6$ |
| formula wt | 1621.76 | 1639.78 | 3441.47 | 3446.74 | 1216.61 | 1625.57 |
| cryst syst | monoclinic | monoclinic | monoclinic | monoclinic | triclinic | monoclinic |
| space group | $P2_1/c$ | $P2_1/c$ | $P2_1/n$ | $Cc$ | $P1$ | $P2_1/n$ |
| $a$ (Å) | 11.6196(7) | 11.6295(5) | 16.2737(6) | 25.061(1) | 10.9605(6) | 7.793(2) |
| $b$ (Å) | 13.8378(7) | 13.8839(7) | 25.412(1) | 14.2632(8) | 13.4534(7) | 15.172(1) |
| $c$ (Å) | 24.514(1) | 24.602(1) | 21.1218(8) | 25.987(2) | 13.4631(7) | 17.927(2) |
| $\alpha$ (deg) | 90 | 90 | 90 | 90 | 89.678(4) | 90 |
| $\beta$ (deg) | 95.817(5) | 96.339(4) | 92.800(3) | 103.035(7) | 89.152(4) | 113.34 (1) |
| $\gamma$ (deg) | 90 | 90 | 90 | 90 | 89.445(4) | 90 |
| $V$ (Å$^3$) | 3921.3(3) | 3948.0(3) | 8724.4(6) | 9049.7(10) | 1984.87(18) | 4443.5 (8) |
| $Z$ | 4 | 4 | 4 | 4 | 2 | 4 |
| $\mu$ (mm$^{-1}$) | 8.19 | 8.14 | 6.66 | 6.24 | 5.19 | 6.96 |
| temp (K) | 150 | 150 | 120 | 110 | 100 | 150 |
| no. of measd rflns | 54223 | 72453 | 117839 | 39250 | 51460 | 32684 |
| no. of indep rflns ($R_{int}$) | 10040 (0.055) | 10195 (0.059) | 22316 (0.059) | 19944 (0.053) | 10083 (0.00) | 10718 (0.087) |
| no. of data/ restraints/paras | 10040/0/317 | 10195/108/325 | 22193/73/730 | 19944/17/695 | 10083/12/334 | 10718/30/388 |
| goodness of fit | 0.96 | 0.97 | 1.01 | 1.00 | 0.99 | 0.99 |
| $R$ ($F^2 > 2\sigma(F^2)$) | 0.050 | 0.113 | 0.050 | 0.057 | 0.091 | 0.076 |
| $R_w$ ($F^2$) | 0.107 | 0.203 | 0.089 | 0.156 | 0.226 | 0.160 |
| residual e$^-$ density (e Å$^{-1}$) | −1.98 to +30.4 | −4.25 to +6.25 | −3.76 to +4.55 | −3.50 to +4.38 | −4.86 to +4.45 | −2.51 to +3.76 |
| CCDC no. | 1017220 | 1017221 | 1017222 | 1017223 | 1017224 | 1017225 |

| | 6 | 7 | 8 | 9 | 10 | 11 |
|---|---|---|---|---|---|---|
| empirical formula | $C_{18}H_{44}BaO_{10}\cdot Cu_4I_6$ | $C_{42}H_{94}Ag_8Ba_2I_{12}O_{21}$ | $C_{40}H_{88}Ag_4Ba_2I_8O_{20}$ | $C_{12}H_{36}BaO_6S_6\cdot Ag_2Cu_2I_6$ | $C_{40}H_{88}Ba_2O_2\cdot CuAg_7I_{12}\cdot C_2H_6O$ | $C_{20}H_{44}BaO_{10}\cdot PbAgI_5\cdot 2C_3H_6O$ |
| formula wt | 1573.46 | 3595.68 | 2610.52 | 1710.40 | 3551.36 | 1647.65 |
| cryst syst | trigonal | monoclinic | monoclinic | monoclinic | monoclinic | monoclinic |
| space group | $R3c$ | $P2_1/n$ | $P2_1/c$ | $P2_1/c$ | $P2_1/n$ | $P2_1/n$ |
| $a$ (Å) | 14.8950(7) | 13.0917(4) | 17.2402(8) | 11.6736 (8) | 13.1013(2) | 14.1172(6) |
| $b$ (Å) | 14.8950(7) | 24.9736(7) | 18.859(1) | 14.0621 (9) | 24.9518(5) | 21.1779(4) |
| $c$ (Å) | 30.693(2) | 26.3839(8) | 22.504(1) | 24.527 (2) | 26.3743(6) | 15.9279(7) |
| $\alpha$ (deg) | 90 | 90 | 90 | 90 | 90 | 90 |
| $\beta$ (deg) | 90 | 91.062(3) | 93.897(4) | 98.095 (7) | 91.368(3) | 95.517(4) |
| $\gamma$ (deg) | 120 | 90 | 90 | 90 | 90 | 90 |
| $V$ (Å$^3$) | 5897.3(5) | 8624.7(4) | 7299.9(6) | 3986.1 (5) | 8620.4(3) | 4739.9(4) |
| $Z$ | 6 | 4 | 4 | 4 | 4 | 4 |
| $\mu$ (mm$^{-1}$) | 7.87 | 7.02 | 5.55 | 7.97 | 7.04 | 8.07 |
| temp (K) | 110 | 110 | 150 | 150 | 150 | 150 |
| no. of measd rflns | 14636 | 117842 | 79199 | 54433 | 120073 | 57037 |
| no. of indep rflns ($R_{int}$) | 1732 (0.079) | 22132 (0.102) | 18257(0.095) | 10178 (0.054) | 22140 (0.063) | 12042 (0.050) |
| no. of data/ restraints/paras | 1732/52/111 | 22089/345/767 | 18218/339/667 | 10178/317/12 | 22093/459/767 | 12017/51/415 |
| goodness of fit | 0.99 | 1.05 | 0.94 | 0.95 | 1.00 | 0.98 |
| $R$ ($F^2 > 2\sigma(F^2)$) | 0.038 | 0.102 | 0.067 | 0.049 | 0.070 | 0.044 |
| $R_w$ ($F^2$) | 0.083 | 0.247 | 0.131 | 0.134 | 0.169 | 0.079 |
| residual e$^-$ density (e Å$^{-1}$) | −2.03 to +3.38 | −4.73 to +6.18 | −4.59 to +3.94 | −3.76 to +5.16 | −3.73 to +2.85 | −3.56 to +4.03 |
| CCDC no. | 1017226 | 1017227 | 1017228 | 1017229 | 1017230 | 1017231 |

1721w, 1627m, 1575w, 1453m, 1342m, 1297w, 1192m, 1089s, 1056s, 1037m, 945m, 862w, 844s, 836w, 533w, 483w.

**X-ray Crystallography.** Suitable crystals of **1−11** were selected and mounted on a Gemini kappa-geometry diffractometer (Agilent Technologies UK Ltd.) equipped with an Atlas CCD detector and using Mo radiation ($\lambda$ = 0.71073 Å). Intensities were collected at low temperature (100, 110, 120, or 150 K) by means of the CrysalisPro software.[9] Reflection indexing, unit-cell parameter refinement, Lorentz−polarization correction, peak integration, and background determination were carried out with the CrysalisPro software.[9] An analytical absorption correction was applied using the modeled faces of the crystal.[10] The resulting set of *hkl* was used for structure solution and refinement. The structures were solved by direct methods with SIR97,[11] and the least-squares refinement on $F^2$ was achieved with the CRYSTALS software.[12] All non-hydrogen atoms were refined anisotropically. The hydrogen atoms were all located in a difference map, but those attached to carbon atoms were repositioned geometrically. The H atoms were initially refined with soft restraints


dx.doi.org/10.1021/ic501963y | *Inorg. Chem.* 2014, 53, 11721−11731

**Scheme 1. Synthesis of 1−11**

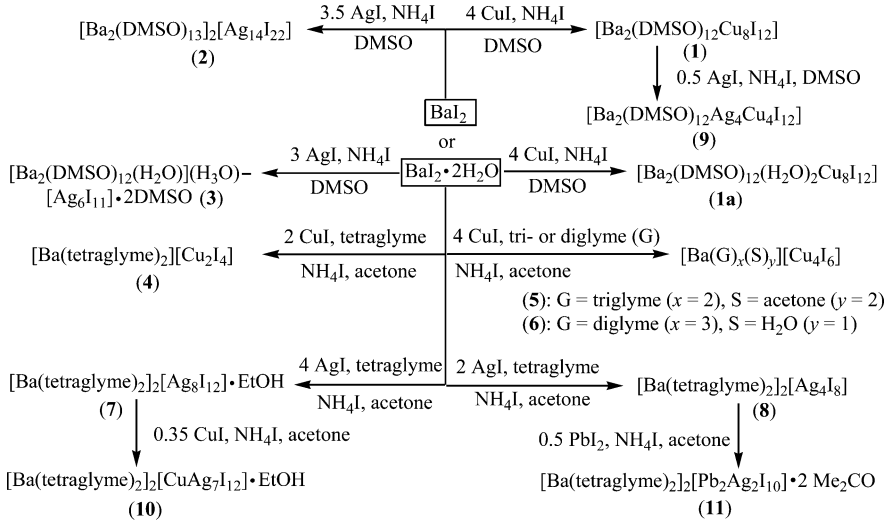


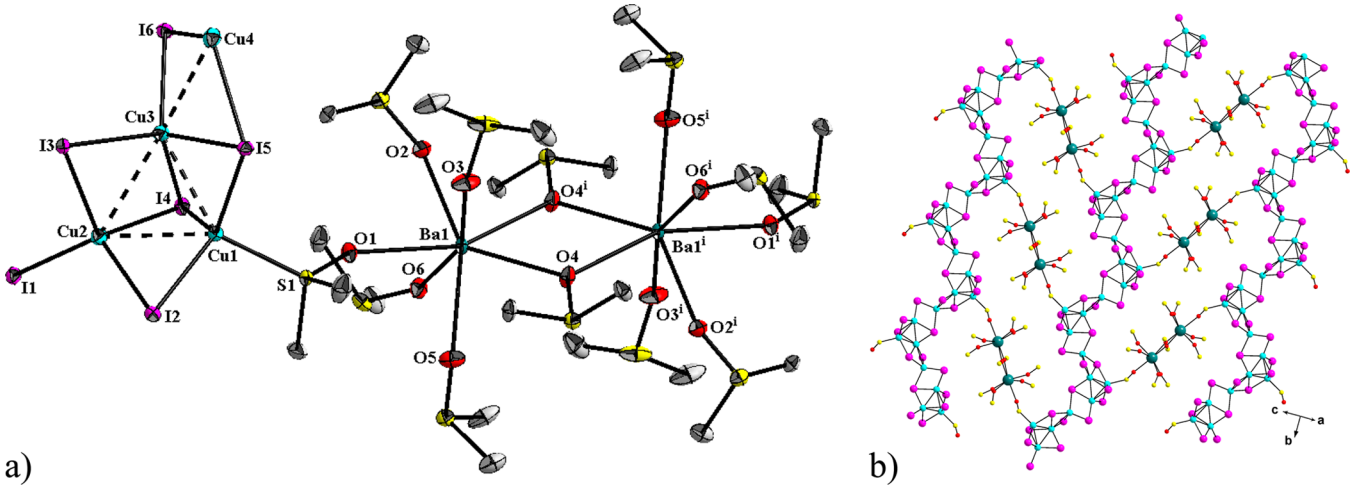


**Figure 1.** (a) Perspective view of $[Ba_2(DMSO)_{12}Cu_8I_{12}]$ (**1**) with 30% probability ellipsoids. H atoms on DMSO ligands are omitted for clarity. (b) Extended structure of **1**.

on the bond lengths and angles to regularize their geometry (C−H in the range 0.93−0.98 Å) and $U_{iso}$(H) (in the range 1.2−1.5 × $U_{eq}$ of the parent atom), after which the positions were refined with riding constraints. Selected crystallographic and refinement data of iodocuprates **1**−**11** are given in Table 1.

## RESULTS AND DISCUSSION

Exploiting a well-known fact that the soft and large iodide anion in barium iodide undergoes autoionization in the presence of many coordinating solvents[13] and hence can be used for the construction of interesting iodometalate fabrics under suitable conditions, we chose to introduce barium−organic complexes for iodocuprates and -argentates. Our interest in these barium-containing iodometalates was also related to their potential use as single-source precursors in materials science. Indeed, barium is an important constituent of many high-tech materials,[14] and it has been shown previously that an all-iodide route to high-$T_c$ $YBa_2Cu_3O_{7-x}$ (YBCO) represents a means to avoid formation of stable $BaCO_3$,[15] which is detrimental to superconductivity. To date, however, very few Ba−Cu iodide heterometallics are known.[16] We chose dimethyl sulfoxide (DMSO) and acyclic polyethers (di-, tri-, and tetraglyme) as ligands to design our metal−organic complexes because they not only ionize iodide anion (completely or partially) but also show interesting and versatile coordination modes (Scheme 1). The DMSO is a well-known ambidentate ligand which can coordinate to a hard metal ions via the oxygen atom, a soft metal ion via the sulfur atom, or a metal ion with borderline coordination properties via either the oxygen or sulfur atom.[17] Rarely, however, it can also act as a bidentate ligand, depending on the electronic features and the steric conditions. In contrast, the chelating nature of the polydentate glyme ligands is well-established. These ligands tend to shield the metal cations very well and saturate their coordination spheres, resulting in stable species. Pioneer work from Fromm has established the structural diversity among the group 2 metal iodide complexes with glyme and related ligands.[13] We have previously reported the remarkable supramolecule $[Ba(tetraglyme)_2]I_2{\cdot}C_7H_8$, which has $Z' = 8$ and a total of 32 unique molecules in the asymmetric unit with a unit cell volume of nearly 15000 Å$^3$.[18]

Irrespective of the molar ratio used, the reaction of $BaI_2$ and CuI in DMSO in the presence of $NH_4I$ yielded colorless crystals of $[Ba_2(DMSO)_{12}Cu_8I_{12}]$ (**1**). The structure of **1** shows versatile bonding modes for the dimethyl sulfoxide ligand, which acts not only in a terminal $\eta^1$(O) or bridging $\mu,\eta^1{:}\eta^1$(O)


dx.doi.org/10.1021/ic501963y | Inorg. Chem. 2014, 53, 11721−11731

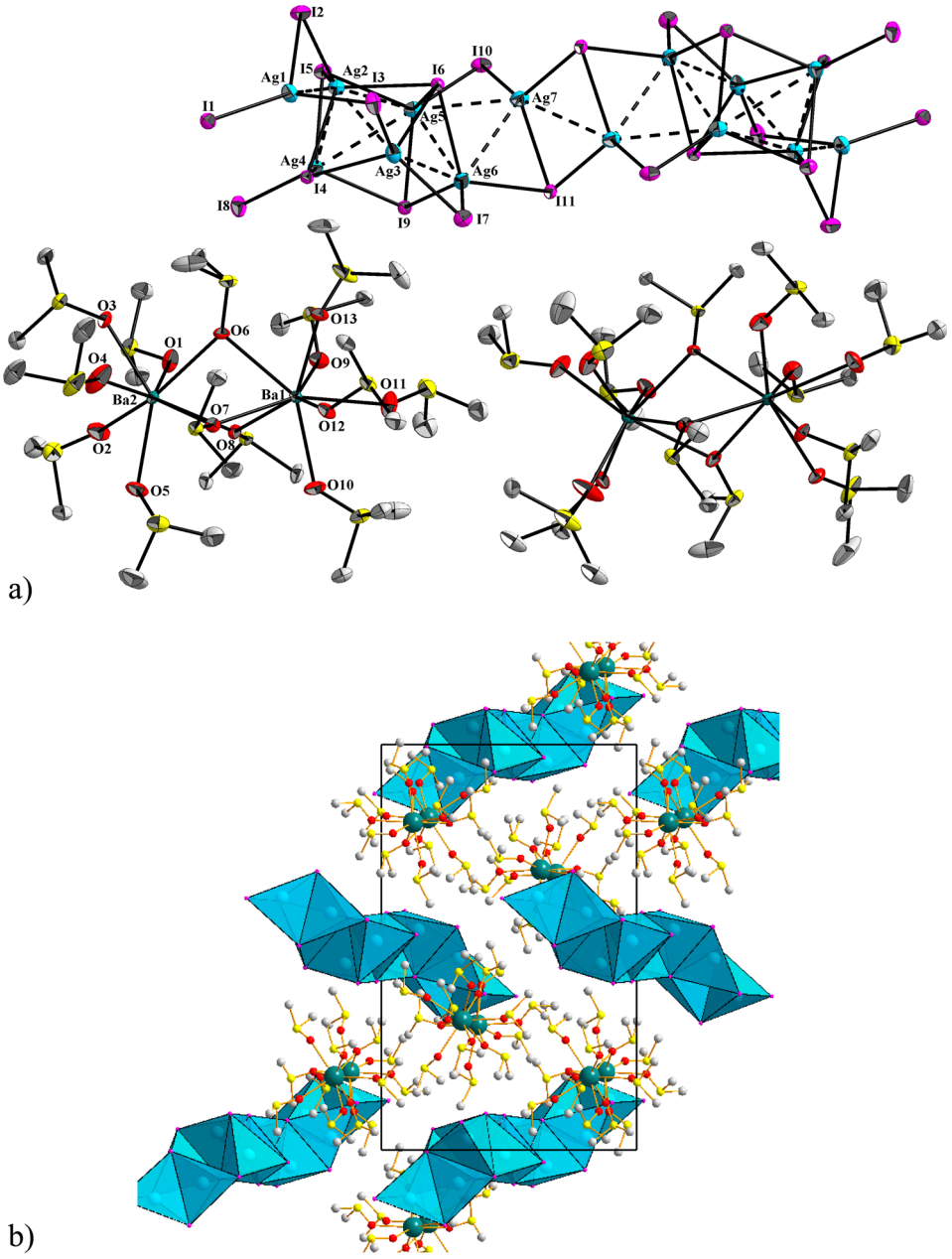


**Figure 2.** (a) Perspective view of $[Ba_2(DMSO)_{13}]_2[Ag_{14}I_{22}]$ (**2**) with 30% probability ellipsoids. H atoms on DMSO ligands are omitted for clarity. (b) Packing structure of **2**.

fashion but also in a amphidentate $\mu,\eta^1{:}\eta^1$(O,S) manner to bind two different metal centers with different acidities (Ba and Cu) to afford heterometallics (Figure 1). The barium dimer $[Ba_2(DMSO)_{12}]^{4+}$ bridged by two $\mu,\eta^1{:}\eta^1$-DMSO groups has seven-coordinate metal centers with capped-trigonal-prismatic geometry. The Ba−O bond lengths range from 2.650(7) to 2.815(7) Å, the Ba−$\mu$-O bonds (average 2.815 Å) being slightly longer than the corresponding Ba−$\eta^1$-O bonds (average 2.682 Å). One of the oxygen-coordinated DMSO ligands on each barium center (Ba1−O1 2.692(7) Å) is also connected to the Cu center via sulfur (Cu1−S1 2.357(2) Å), thus providing a proper bonding between the barium−organic complex and the iodocuprate moiety. The tetranuclear $[Cu_4(\mu_3\text{-}I)_3(\mu\text{-}I)_3]^{2-}$ units comprised of $CuI_4$ or $CuI_3S$ tetrahedra are associated into zigzag chains (angle 62.2(3)°) via an edge-sharing arrangement, leading iodide ligands to be in either a $\mu_3$ or $\mu$ bridging mode (Figure 1 and Figure S2 (Supporting Information)). As expected, the average Cu−I bond distances are larger for $\mu_3$-I (2.920 Å) than for $\mu$-I (2.815 Å). The I−Cu−I bond angles vary from 95.58(4) to 144.86(4)°, deviating significantly from 109.5° for an ideal tetrahedron (Table S1 (Supporting Information)). Apart from the bridging iodides, the construction of 1D zigzag chain is also helped by the cuprophilic Cu(I)···Cu(I) interactions, the distances ranging from 2.680(2) to 2.930(2) Å. The two adjacent zigzag chains are arranged in such a manner that they form an incomplete ringlike structure. Each of these rings encapsulates a $[Ba_2(DMSO)_{12}]^{4+}$ cation, actually a template that is connected with the iodocuprate moiety via Cu−S−O−Ba bonds; thus, a 2D sheetlike structure is obtained. We have previously observed that by gradual introduction of water molecules in the metal−organic complex, and thus H bonding between the metal−


dx.doi.org/10.1021/ic501963y | Inorg. Chem. 2014, 53, 11721−11731

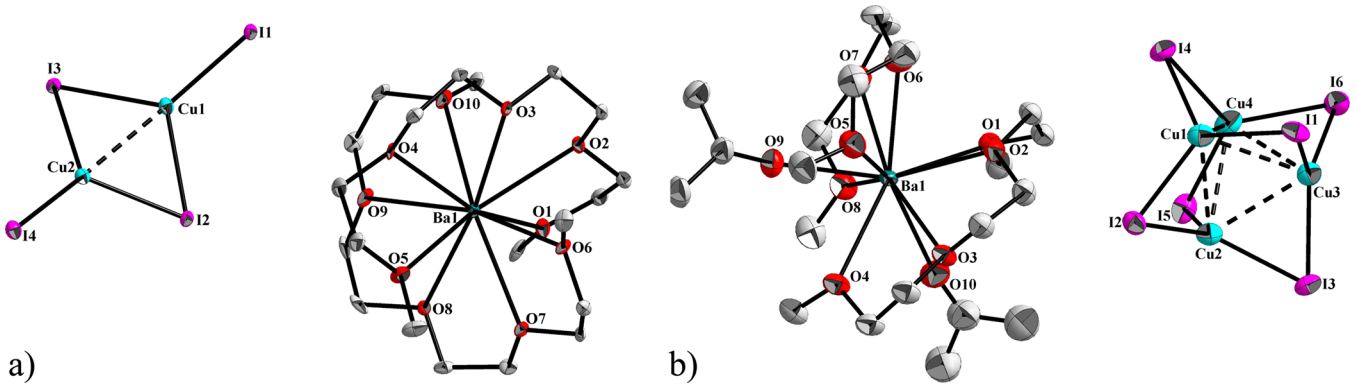


**Figure 3.** Perspective views of (a) $[Ba(tetraglyme)_2][Cu_2I_4]$ (**4**) and (b) $[Ba(triglyme)_2(acetone)_2][Cu_4I_6]$ (**5**) with 30% probability ellipsoids. H atoms on the glyme ligands are omitted for clarity.

organic complex and iodocuprate moieties, it is possible to increase the dimensionality of the iodocuprate clusters and finally obtain 3D porous metal−organic frameworks.[5] We were curious as to whether introduction of $H_2O$ in the barium−organic moiety could bring in another dimensionality in the overall structure of **1**. In view of this, we modified the synthesis of **1** slightly and used hydrated $BaI_2{\cdot}2H_2O$ as the starting reactant. This indeed led to incorporation of water molecules in the coordination sphere of the barium−organic complex, thus changing the coordination number of the Ba atom to 8 and the geometry to distorted dodecahedral. However, the iodocuprate moiety in the resulting $[Ba_2(DMSO)_{12}(H_2O)_2Cu_8I_{12}]$ (**1a**) was unchanged (Figure S3 (Supporting Information)).

Similar reactions of $BaI_2$ and $BaI_2{\cdot}2H_2O$ with AgI in DMSO produced $[Ba_2(DMSO)_{13}]_2[Ag_{14}I_{22}]$ (**2**) and $[Ba_2(DMSO)_{12}(H_2O)](H_3O)[Ag_6I_{11}]{\cdot}2DMSO$ (**3**), respectively. Unlike the Ba($\mu$-DMSO)$_2$Ba moiety in **1** and **1a**, the dinuclear barium cations here are formed by three bridging DMSO ligands. In **2**, the charge balance for two such dinuclear barium cations is provided by a tetradecanuclear $[Ag_{14}(\mu_5\text{-}I)_2(\mu_4\text{-}I)_2(\mu_3\text{-}I)_6(\mu\text{-}I)_8I_4]^{8-}$ cluster built from the characteristic edge-sharing $AgI_4$ tetrahedra (Figure 2 and Figure S4 (Supporting Information)). The structure of the asymmetric unit $[Ag_7(\mu_5\text{-}I)(\mu_4\text{-}I)(\mu_3\text{-}I)_3(\mu\text{-}I)_4I_2]^{4-}$ can be viewed as built up from a distorted pseudocubane connected additionally by three $AgI_4$ tetrahedra. In the distorted pseudocubane, the bond Ag3−I9 (4.872 Å) opens up a bit to accommodate an additional Ag(6)$I_4$ tetrahedron, which is connected via two common edges (I6 and I7 with Ag3 and I6 and I9 with Ag5). Two additional $AgI_4$ tetrahedra are connected with this pseudocubane to complete the asymmetric $Ag_7I_{11}$ unit: Ag(1)$I_4$ (via I3 and I4 with Ag3 and I2 and I4 with Ag2) and Ag(7)I4 (via I6 and I10 with Ag5 and I6 and I11 with Ag6). Two such asymmetric units connect through the common edge I7, I7′ to afford a discrete $Ag_{14}$ cluster. As a consequence of the connectivity of $AgI_4$ tetrahedra, the iodide ligands act in a versatile manner, the bonding varying from quintuply bridging (I6) to quadruply bridging (I4), triply bridging (I5, I9, I11), doubly bridging (I2, I3, I7, I10), and terminal ligands (I1, I8) and the average Ag−I bond distances decreasing gradually from 3.006 to 2.965, 2.868, 2.787, and 2.741 Å for $\mu_5$-I, $\mu_4$-I, $\mu_3$-I, $\mu$-I, and terminal-I, respectively. It should be noted that a hypercoordination number of iodide as high as $\mu_{12}$ has recently been reported.[19] The argentophillic Ag···Ag distances, 3.164(1)−3.599(1) Å, compare well with the body of literature.[5] To our knowledge, the unprecedented $[Ag_{14}I_{22}]^{6-}$ cluster is the largest discrete iodoargentate reported so far. In contrast to the case for **2**, there are two different cations, $[Ba_2(DMSO)_{12}(H_2O)]^{4+}$ and $[H_3O]^+$, to balance the charge of hexanuclear iodoargentate $[Ag_6I_{11}]^{5-}$ anions in **3**. The anion $[Ag_6(\mu_4\text{-}I)_2(\mu_3\text{-}I)_3(\mu\text{-}I)I_5]^{5-}$ in **3** can be viewed as built from a fusion of two pseudocubanes through the common face Ag3−I6−Ag4−I7 (Figure S5 (Supporting Information)). One of the cubanes is highly distorted, as one bond Ag4−I11 opens up a bit to have a long distance of 4.006 Å. The opening of this bond is, however, compensated by an additional terminal I on Ag4, which ensures a $AgI_4$ tetrahedron. There is also one terminal iodide on each of the four peripheral Ag atoms to complete a tetrahedral environment around them. In addition to terminal iodides (I1, I3, I8, I9, and I10), there are different types of bridging iodides which ensure connectivity between these $AgI_4$ tetrahedra: $\mu_4$ (I6, I7), $\mu_3$ (I2, I4, I5), and $\mu$ (I11). The $[Ag_6I_{11}]^{5-}$ cluster reported here represents a new structural motif for hexanuclear iodoargentate compositions, which is very different from that for the discrete $[Ag_6(\mu_4\text{-}I)_3(\mu_3\text{-}I)_2(I)_6]^{5-}$ anion, where the core of $Ag_6$ forms a trigonal prism.[20]

The reaction of $BaI_2{\cdot}2H_2O$ with CuI in acetone in the presence of glyme ligands gave hybrid complexes with discrete iodocuprate clusters and glyme-wrapped barium cations. In $[Ba(tetraglyme)_2][Cu_2I_4]$ (**4**), the barium ion is coordinated by 10 oxygen atoms of 2 tetraglyme ligands, the 5 oxygen atoms of each tetraglyme ligand lying approximately in a plane. The planes of the two tetraglymes are inclined to each other by 86.32(6)°. The Ba−O(tetraglyme) bond lengths (average 2.87 Å) are comparable to the literature values.[18] The charge balance for this cation is provided by a dinuclear $[Cu_2(\mu\text{-}I)_2I_2]^{2-}$ cluster (Figure 3). This relatively planar cluster has two trigonal-planar Cu(I) centers bridged by two $\mu$-I atoms with each center having one terminal iodide ligand. As expected, the Cu−$\mu$-I (average 2.60 Å) bond distances are longer than the terminal Cu−I distances (average 2.52 Å). The Ba atoms in $[Ba(triglyme)_2(acetone)_2][Cu_4I_6]$ (**5**) (Figure 3) and $[Ba(diglyme)_3(H_2O)][Cu_4I_6]$ (**6**) (Figure S6 (Supporting Information)) are also 10-coordinated. The $[Cu_4I_6]^{2-}$ cluster in **5** and **6** consists of a tetrahedron of Cu atoms bridged on each edge by the six I atoms. The Cu atoms are three-coordinate, with average Cu−I distances of 2.612(3) and 2.561(2) Å in **5** and **6**, respectively. The average cuprophilic Cu···Cu distance in **5** and **6**, 2.762 Å, is slightly longer than that found in **4** (2.636 Å). While the tetrahedral $[Cu_4I_6]^{2-}$ cluster has been described previously,[21] the dinuclear $[Cu_2(\mu\text{-}I)_2I_2]^{2-}$ cluster has no precedent in the literature.


dx.doi.org/10.1021/ic501963y | Inorg. Chem. 2014, 53, 11721−11731

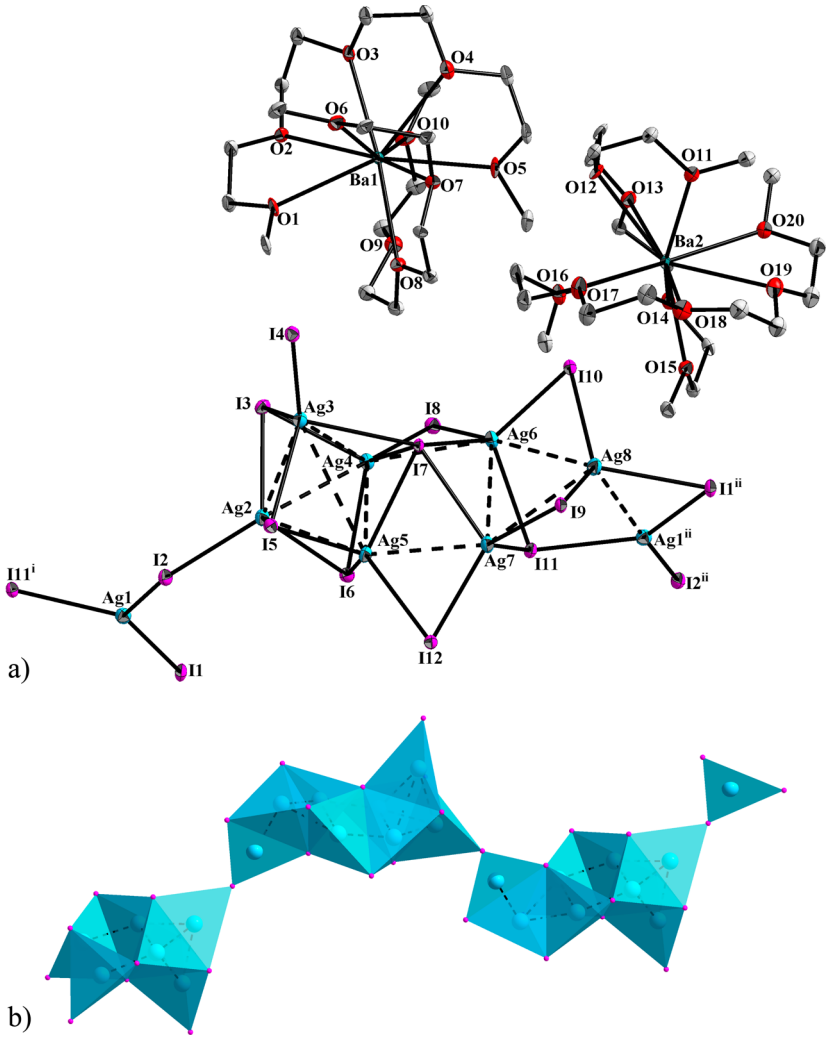


**Figure 4.** (a) Perspective view of $[Ba(tetraglyme)_2]_2[Ag_8I_{12}]\cdot EtOH$ (**7**) with 30% probability ellipsoids. H atoms on tetraglyme ligands and EtOH molecules are omitted for clarity. (b) Polyhedral representation of the iodoargentate chain. Symmetry elements: (i) $^5/_2 - x, y - {}^1/_2, {}^1/_2 - z$; (ii) $^5/_2 - x, {}^1/_2 + y, {}^1/_2 - z$.

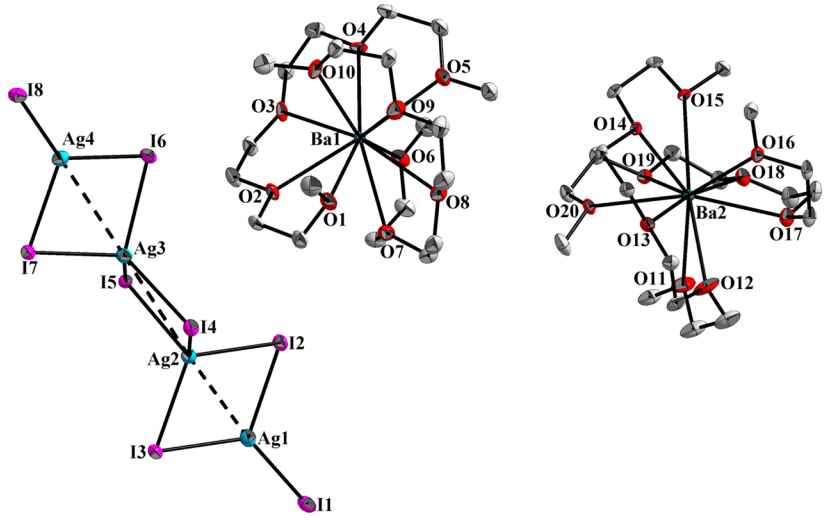


**Figure 5.** Perspective view of $[Ba(tetraglyme)_2]_2[Ag_4I_8]$ (**8**) with 30% probability ellipsoids. H atoms on the tetraglyme ligand are omitted for clarity.

Depending upon the molar ratios of the reactants used and the crystallization conditions, the reaction of $BaI_2\cdot 2H_2O$ with AgI in acetone in the presence of tetraglyme and $NH_4I$ resulted in two different products. While the reaction of $BaI_2\cdot 2H_2O$ with 4 equiv of AgI, followed by layering of the acetone solution with ethanol at room temperature, gave [Ba-


dx.doi.org/10.1021/ic501963y | *Inorg. Chem.* 2014, 53, 11721−11731

(tetraglyme)$_2$]$_2$[Ag$_8$I$_{12}$]·EtOH (**7**), a similar reaction in 1:2 molar ratio, followed by crystallization with a acetone/toluene mixture, gave [Ba(tetraglyme)$_2$]$_2$[Ag$_4$I$_8$] (**8**). In the structure of **7**, the [Ag$_8$I$_{12}$]$^{4-}$ building block of an overall 1D zigzag iodoargentate chain has two [Ba(tetraglyme)$_2$]$^{2+}$ cations to balance the charge (Figure 4). While the helically wrapped [Ba(tetraglyme)$_2$]$^{2+}$ cation is more or less similar to that in **4**, the zigzag [Ag$_8$I$_{12}$]$^{4-}$ moiety can be described as two pseudocubanes joined through the common vertex $\mu_5$-I (I7) and two $\mu$-I atoms (I8 and I12). One missing Ag distorts one of the cubanes considerably. This disorted cubane is additionally connected to the planar triangle Ag(1)I$_3$ via one $\mu_4$-I(11) and one $\mu$-I(1) to complete the octanuclear building block. These octanuclear building blocks are joined through $\mu$-I to form a zigzag linear structure (Figure S7 (Supporting Information)). As a consequence of the connectivity of seven AgI$_4$ tetrahedra via edge sharing and one AgI$_3$ triangle plane via vertex sharing, the iodide ligands are connected in a versatile manner: $\mu_5$-I (I7), $\mu_4$-I (I1), $\mu_3$-I (I3, I5, I6), $\mu$-I (I1, I2, I8, I9, I10, I12), and terminal (I4). The average Ag−I bond distances increase from 2.734 to 2.790, 2.883, 2.967, and 2.994 Å as the connectivity of iodides increases from one to five, respectively. Similar to the case for **7**, there are two [Ba(tetraglyme)$_2$]$^{2+}$ cations to balance the charge of the tetranuclear iodoargentate [Ag$_4$I$_8$]$^{4-}$ anion in [Ba(tetraglyme)$_2$]$_2$[Ag$_4$I$_8$] (**8**), though the iodoargentate anion is a discrete tetranuclear Ag$_4$I$_8$ moiety (Figure 5). This cluster can be viewed as built from edge-sharing of two central AgI$_4$ tetrahedra and two peripheral AgI$_3$ planar triangles, if the Ag···Ag interactions are not taken into account. The peripheral planar triangles Ag(1)I$_3$/Ag(4)I$_3$ are connected to the central tetrahedra Ag(2)I$_4$/Ag(3)I$_4$ via the common edges I(2)−I(3)/I(6)−I(7) to generate two Ag$_2$I$_5$ units which, in turn, are connected by the common edge I(4)−I(5) to afford a linear tetranuclear [Ag$_4$($\mu$-I)$_6$I$_2$]$^{4-}$ anion.

As outlined in the Introduction, the basic idea of the synthesis of the above iodometalates was to see whether these can serve as templates for constructing rare metal−organic incorporated heterometallic iodometalates containing three different metals. For this purpose, complexes **1** and **7** were further reacted with calculated amounts of AgI and CuI, respectively, in a suitable solvent (DMSO or acetone) in the presence of NH$_4$I. The colorless complexes isolated after layering the respective reaction solutions with ethanol contained both copper and silver, as first indicated by the elemental analysis and further confirmed by the X-ray structures of the isolated complexes [Ba$_2$(DMSO)$_{12}$Cu$_4$Ag$_4$I$_{12}$] (**9**) and [Ba(tetraglyme)$_2$]$_2$[CuAg$_7$I$_{12}$]·EtOH (**10**), respectively. Their structures are identical with those of **1** and **7**, respectively, except that half of the copper atoms have been replaced by silver atoms in **9** (Figure 6 and Figure S8 (Supporting Information)), whereas one silver atom was replaced with a copper atom in **10** (Figure 7 and Figure S9 (Supporting Information)). It is worth noting that the replaced copper atoms in **9** are those which had a longer Cu···Cu distance (2.740 Å) with the copper atom (Cu1) bonded to the barium cation via a sulfur atom. The average distance for the mixed metallophilic Cu···Ag interaction (2.806 Å) in **9** is between those found for Cu···Cu (2.771 Å) and Ag···Ag (3.277 Å) interactions. In **10**, on the other hand, the replacement of the tricoordinate Ag1 with a copper atom was preferred over tetrahedrally connected silver atoms. As expected, the replacement of Ag1 with the smaller copper atom causes shortening of the metal−iodide bonds (2.527(2)−2.601(2) Å

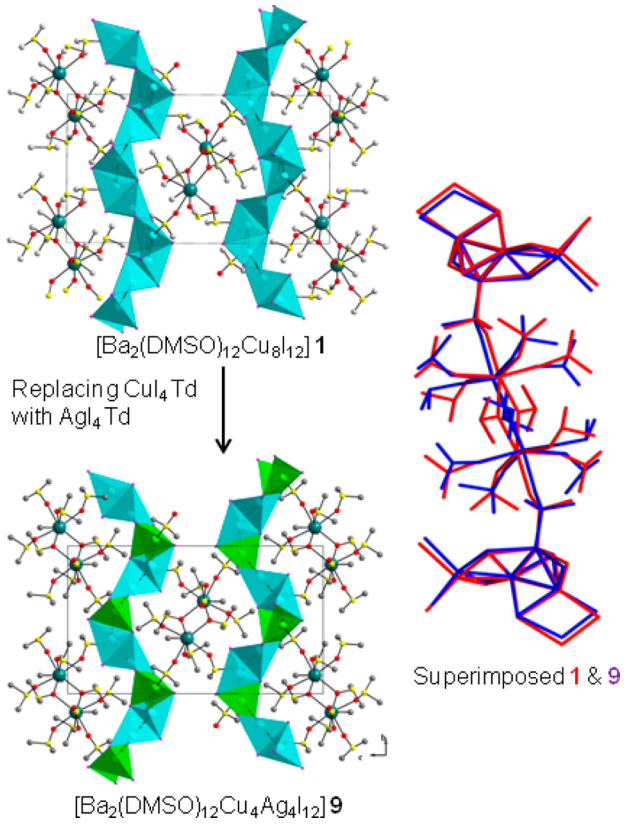


**Figure 6.** Synthesis of the novel heterotrimetallic **9** starting from the bimetallic precursor **1**. The superimposed figure shown on the right underlines the template properties of the precursor **1** during the synthesis of **9**.

for CuI$_3$ in **10** as opposed to 2.690(3)−2.773(3) Å for AgI$_3$ in **7**), though this difference is less pronounced in the mixed metallophilic Cu···Ag interaction (2.989(2) Å in **10** in comparison to the Ag···Ag distance, 3.038(4) Å, found in the precursor **7**).

In contrast to the template effect found for the above mixed Cu−Ag iodometalates **9** and **10**, the reaction of **8** with PbI$_2$ in acetone yielded the mixed Ag−Pb iodometalate [Ba(tetraglyme)$_2$]$_2$[Pb$_2$Ag$_2$I$_{10}$]·2Me$_2$CO (**11**), where the basic structure of the precursor [Ba(tetraglyme)$_2$]$_2$[Ag$_4$I$_8$] (**8**) was not retained. This breakdown in the structure-directing properties of the metal−organic-containing iodoargentate **8** could be attributed to the molecular rearrangement required as a result of replacing AgI$_4$/AgI$_3$ units with octahedral PbI$_6$ units. The molecular structure of **11** is composed of a [Ba(tetraglyme)$_2$]$^{2+}$ cation and the discrete mixed Ag−Pb iodometalate anions formed by edge- and face-sharing AgI$_4$ tetrahedra and PbI$_6$ octahedra (Figure 8 and Figure S10 (Supporting Information)). The mixed Ag−Pb iodometalate moiety Ag$_2$Pb$_2$I$_{10}$$^{4-}$ contains a butterfly [Ag$_2$Pb$_2$($\mu_3$-I)$_2$($\mu$-I)$_2$I$_4$]$^{2-}$ core in which the two Ag$^+$ ions act as the "body" and two Pb$^{2+}$ ions as "wings". The two Ag$^+$ ions are held together with two outer Pb$^{2+}$ ions by two $\mu_4$-I and four $\mu$-I groups. Two terminal iodides on each lead atom then complete the six-coordination environment around it. The Ag···Ag distance is 3.8312(5) Å.

**Luminescence Properties.** Among the hybrid complexes reported here, iodometalates **2** and **4**−**6** show intense luminescence in the solid state, while the iodoargentate **8** is only weakly emissive. For each luminescent sample, a complete


dx.doi.org/10.1021/ic501963y | Inorg. Chem. 2014, 53, 11721−11731

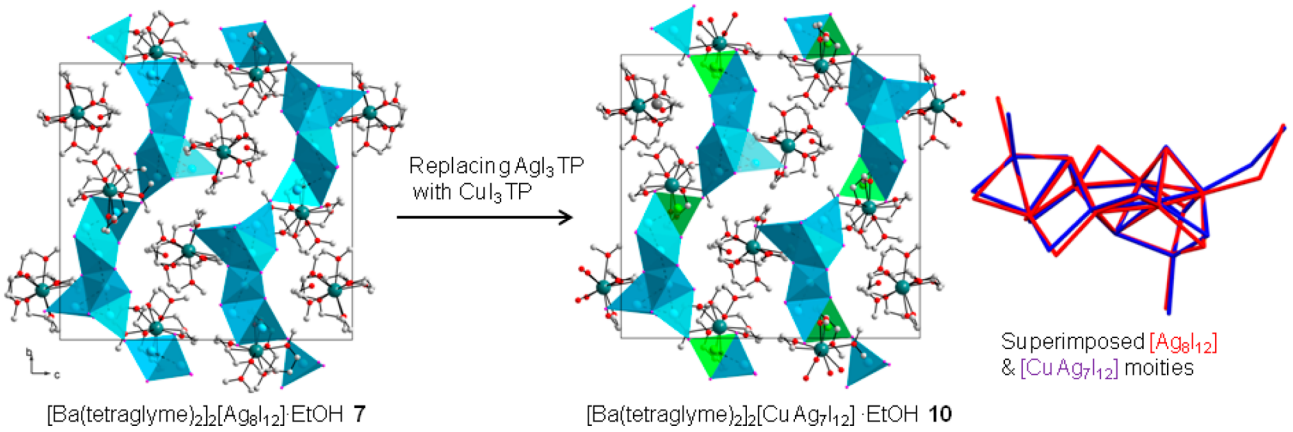


**Figure 7.** Synthesis of the novel heterotrimetallic **10** starting from the bimetallic precursor **7**. The superimposed figure shown on right underlines the template properties of the precursor **7** during the synthesis of **10**.

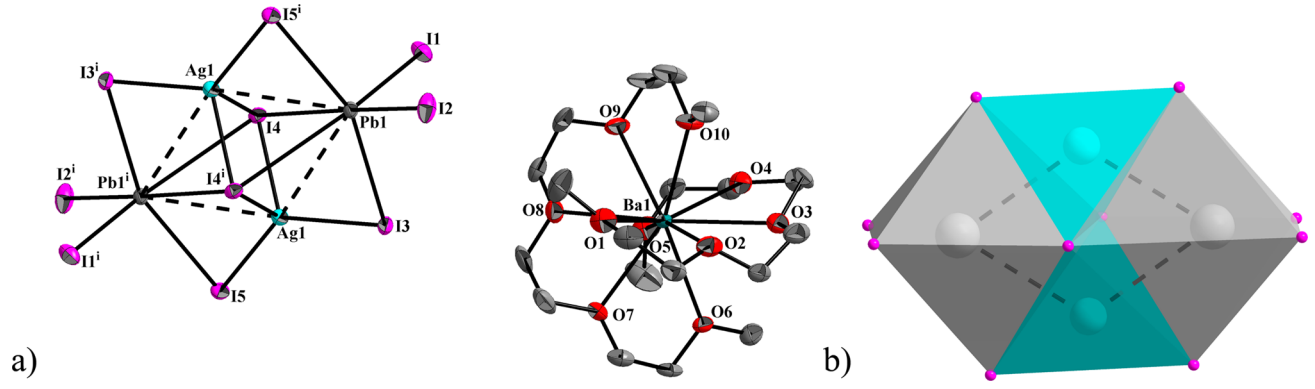


**Figure 8.** (a) Perspective view of $[Ba(tetraglyme)_2]_2[Ag_2Pb_2I_{10}]\cdot 2Me_2CO$ (**11**) with 30% probability ellipsoids. H atoms on the tetraglyme ligands are omitted for clarity. (b) Polyhedral representation of the $[Ag_2Pb_2I_{10}]$ moiety. Symmetry elements: (i) 1-*x*, 1-*y*, -*z*.

mapping in excitation/emission was performed and Figure 9a presents the best excitation and emission cuts of this mapping. The complexes **5** and **6**, which have identical $Cu_4I_6^{2-}$ clusters, present similar luminescence properties and show vivid green fluorescence on exposure to UV light. The iodocuprate cluster **4**, on the other hand, shows bright orange-yellow fluorescence on exposure to UV light. The emission with maxima at about 680, 530, and 450 nm for **4**, **5** (**6**), and **2**, respectively, can be attributed to the cluster-centered (CC) emission, derived from mixed iodide to metal charge transfer (XMCT) and ds/dp metal-centered (MC) excited states.[2] The transitions that give origin to this emission are localized on the metal cluster and can occur only when the M···M (M = Cu, Ag) distance in the cluster is lower than the sum of the orbital interaction radii. The red shift in the emission band of **4** with respect to that of **5** can be related to the shortening of the Cu···Cu distances (2.636 Å in **4** vs 2.762 Å in **5**), giving a higher Cu···Cu bonding character in the CC state. Similar assignments have been suggested and, in some cases, verified by the theoretical calculations for the related hybrid iodocuprates and iodoargentates.[2,5,21] The quantum yield of **2** and **4**–**6** were determined by comparing their luminescent intensities with that of a porous silicon sample (see the Supporting Information for details).[22] Quantum yields of 21 and 69% were calculated for **4** and **5**, respectively, making the latter compound one of the most highly luminescent copper iodide clusters known so far.[2,23] While **6** showed a luminescence intensity comparable with that of **5**, the iodoargentate cluster **2**, with a quantum yield value about 36 times lower than that of **5**, was found to be the weakest among the luminescent compounds reported here. The acetone solutions of these hybrids are amenable to spin/dip

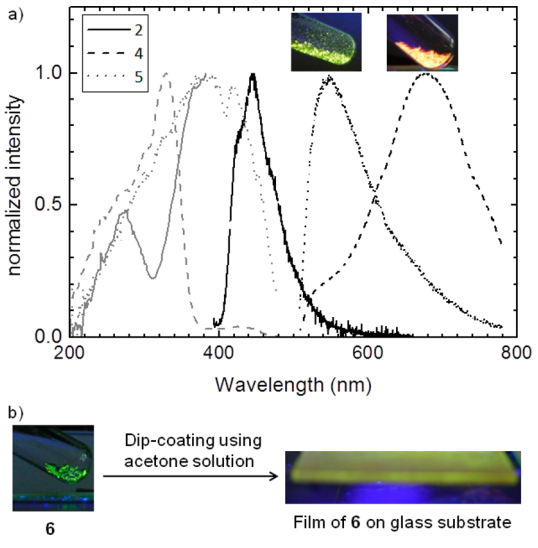


**Figure 9.** (a) Room-temperature solid-state emission and excitation spectra, in black and gray, respectively, of **2**, **4**, and **5**. The colorless iodocuprates show vivid fluorescence on exposure to UV light (digital images shown in inset). (b) Thin film of $[Ba(diglyme)_3(H_2O)][Cu_4I_6]$ (**6**) on a glass substrate by dip coating in acetone solution.


dx.doi.org/10.1021/ic501963y | *Inorg. Chem.* 2014, 53, 11721−11731

coating for the elaboration of thin films on a substrate (Figure 9b), which assumes importance as some of the promising applications of luminescent materials require thin films. The photoluminescent behavior of copper(I) and silver(I) halide clusters is often dependent on their structures,[2] though no clear trend was observed among the hybrids **1**−**11** reported here. While the presence of a water molecule, which is a well-known quencher of luminescence, might be the reason for non-luminescence in **1a** and **3**, it does not explain the luminescence behavior of the hydrated **6**. Similarly, the nonemissive behavior of **11**, which is derived from the luminescent **8** and, like other luminescent derivatives **2** and **4**−**6**, contains a discrete $[Ag_2Pb_2I_{10}]^{4-}$ cluster, is inexplicable. While the weak luminescence properties of **8** are not retained in **11**, the introduction of lead atoms in the iodometalate moiety reduces the band gap from about 3.2 to 2.4 eV, as indicated from the diffuse-reflectance spectra (Figure 10).

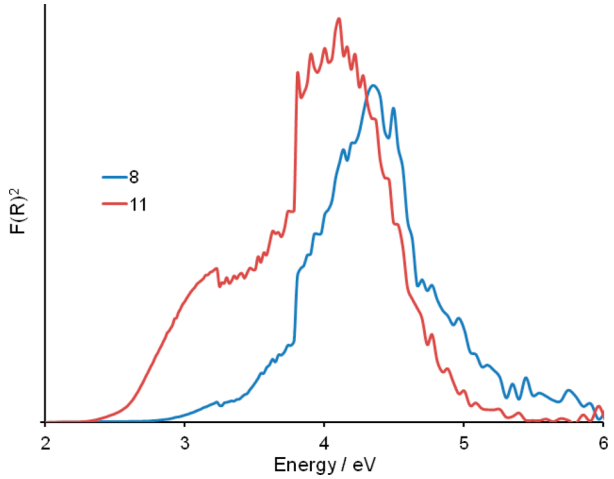


**Figure 10.** Diffuse reflectance spectra of $[Ba(tetraglyme)_2]_2[Ag_4I_8]$ (**8**) and $[Ba(tetraglyme)_2]_2[Ag_2Pb_2I_{10}]\cdot 2Me_2CO$ (**11**).

## CONCLUSIONS

In summary, we have successfully used novel barium−organic-containing iodocuprates and -argentates as templating synthons for constructing rare Ba−Cu−Ag and Ba−Ag−Pb hetero-trimetallic hybrids with interesting structural motifs and topologies. The successful isolation of the barium−organic-containing mixed Ag−Cu iodometalates **9** and **10** not only demonstrates that the replacement of tetrahedral $MI_4$ or a trigonal-planar $MI_3$ unit by another $M'I_4/M'I_3$ unit is a feasible route to synthesize heterometallic halometalates but also shows the structure-directing properties of the precursor derivatives, therefore confirming the significant potential of this strategy, which opens up more possibilities for novel heterotrimetallic compounds with interesting properties.

## ASSOCIATED CONTENT

### Supporting Information

Text, figures, tables, and CIF files giving FT-IR spectra of **1a**, **1**−**6**, and **8**−**11**, perspective view/extended structures and polyhedral representations of **1**, **1a**, **2**, **3**, **6**, **7**, and **9**−**11**, simulated and experimental XRD pattern of selected complexes, experimental part on the quantum yield determination, and selected bond lengths (Å) and angles (deg) for **1**−**11**. This material is available free of charge via the Internet at http://pubs.acs.org.

## AUTHOR INFORMATION

### Corresponding Authors

*S.M.: fax, (+33) 472445399; e-mail, shashank.mishra@ircelyon.univ-lyon1.fr.

*S.D.: e-mail, daniele@ircelyon.univ-lyon1.fr.

### Author Contributions

The manuscript was written through contributions of all authors. All authors have given approval to the final version of the manuscript.

### Notes

The authors declare no competing financial interest.

## ACKNOWLEDGMENTS

The authors thank Y. Aizac and F. Bosselet of IRCELYON for PXRD.

## REFERENCES

(1) See for some recent examples: (a) Estager, J.; Holbrey, J. D.; Swadzba-Kwasny, M. *Chem. Soc. Rev.* **2014**, *43*, 847. (b) Burschka, J.; Pellet, N.; Moon, S.-J.; Humphry-Baker, R.; Gao, P.; Nazeeruddin, M. K.; Gratzel, M. *Nature* **2013**, *499*, 316. (c) Xing, G.; Mathews, N.; Sun, S.; Lim, S. S.; Lam, Y. M.; Grätzel, M.; Mhaisalkar, S.; Sum, T. C. *Science* **2013**, *342*, 344. (d) Liu, Y.; Hu, C.; Comotti, A.; Ward, M. D. *Science* **2011**, *333*, 436. (e) Leblanc, N.; Mercier, N.; Zorina, L.; Simonov, S.; Auban-Senzier, P.; Pasquier, C. *J. Am. Chem. Soc.* **2011**, *133*, 14924. (f) Zhao, H.-R.; Li, D.-P.; Ren, X.-M.; Song, Y.; Jin, W.-Q. *J. Am. Chem. Soc.* **2010**, *132*, 18. (g) Louvain, N.; Mercier, N.; Boucher, F. *Inorg. Chem.* **2009**, *48*, 879.

(2) (a) Perruchas, S.; Le Goff, X. F.; Maron, S.; Maurin, I.; Guillen, F.; Garcia, A.; Gacoin, T.; Boilot, J.-P. *J. Am. Chem. Soc.* **2010**, *132*, 10967. (b) Peng, R.; Li, M.; Li, D. *Coord. Chem. Rev.* **2010**, *254*, 1. (c) Lee, J. Y.; Kim, H. J.; Jung, J. H.; Sim, W.; Lee, S. S. *J. Am. Chem. Soc.* **2008**, *130*, 13838. (d) Tsuboyama, A.; Kuge, K.; Furugori, M.; Okada, S.; Hoshino, M.; Ueno, K. *Inorg. Chem.* **2007**, *46*, 1992. (e) Arnby, C. H.; Jagner, S.; Dance, I. *CrystEngComm* **2004**, *6*, 257.

(3) (a) Lapprand, A.; Bonnot, A.; Knorr, M.; Rousselin, Y.; Kubicki, M. M.; Fortin, D.; Harvey, P. D. *Chem. Commun.* **2013**, *49*, 8848. (b) Kang, Y.; Wang, F.; Zhang, J.; Bu, X. *J. Am. Chem. Soc.* **2012**, *134*, 17881. (c) Mishra, S.; Jeanneau, E.; Daniele, S. *Polyhedron* **2010**, *29*, 500. (d) Zhao, Z.-G.; Zhang, J.; Wu, X.-Y.; Zhai, Q.-G.; Chen, L.-J.; Chen, S.-M.; Xie, Y.-M.; Lu, C.-Z. *CrystEngComm* **2008**, *10*, 273. (e) Bi, M.; Li, G.; Zou, Y.; Shi, Z.; Feng, S. *Inorg. Chem.* **2007**, *46*, 604. (f) Martin, J. D.; Yang, J.; Dattelbaum, A. M. *Chem. Mater.* **2001**, *13*, 392. (g) Martin, J. D.; Greenwood, K. B. *Angew. Chem., Int. Ed.* **1997**, *36*, 2072.

(4) (a) Mishra, S.; Jeanneau, E.; Iasco, O.; Ledoux, G.; Luneau, D.; Daniele, S. *Eur. J. Inorg. Chem.* **2012**, 2749. (b) Goforth, A. M.; Tershansy, M. A.; Smith, M. D.; Peterson, L. R., Jr.; Kelley, J. G.; DeBenedetti, W. J. I.; zur Loye, H.-C. *J. Am. Chem. Soc.* **2011**, *133*, 603. (c) Mishra, S.; Jeanneau, E.; Daniele, S.; Ledoux, G.; Swamy, P. N. *Inorg. Chem.* **2008**, *17*, 9333. (d) Dong, Y.-B.; Smith, M. D.; zur Loy, H.-C. *Angew. Chem., Int. Ed.* **2000**, *39*, 4271.

(5) (a) Mishra, S.; Jeanneau, E.; Ledoux, G.; Daniele, S. *CrystEngComm* **2012**, *14*, 3894. (b) Li, H.-H.; Chen, Z.-R.; Sun, L.-G.; Lian, Z.-X.; Chen, X.-B.; Li, J.-B.; Li, J.-Q. *Cryst. Growth Des.* **2010**, *10*, 1068. (c) Mishra, S.; Jeanneau, E.; Ledoux, G.; Daniele, S. *Dalton Trans.* **2009**, 4954. (d) Mishra, S.; Jeanneau, E.; Daniele, S.; Ledoux, G. *Dalton Trans.* **2008**, 6296. (e) Jiang, Y.-S.; Yao, H.-G.; Ji, S.-H.; Ji, M.; An, Y.-L. *Inorg. Chem.* **2008**, *47*, 3922. (f) Mishra, S.; Jeanneau, E.; Chermette, H.; Daniele, S.; Hubert-Pfalzgraf, L. G. *Dalton Trans.* **2008**, 620. (g) Mishra, S.; Jeanneau, E.; Daniele, S.; Hubert-Pfalzgraf, L. G. *CrystEngComm* **2008**, *10*, 814. (h) Tershansy, M. A.; Goforth, A. M.; Ellsworth, J. M.; Smith, M. D.; zur Loye, H.-C. *CrystEngComm* **2008**,

*10*, 833. (i) Mishra, S.; Hubert-Pfalzgraf, L. G.; Jeanneau, E.; Chermette, H. *Dalton Trans.* **2007**, 410.
(6) (a) Yuan, M.-W.; Li, L.-H.; Chen, L. *Z. Anorg. Allg. Chem.* **2009**, *11*, 1645. (b) Huebner, L.; Kornienko, A.; Emge, T. J.; Brennan, J. G. *Inorg. Chem.* **2004**, *43*, 5659.
(7) (a) Shen, Y.; Lu, J.; Tang, C.; Fang, W.; Jia, D.; Zhang, Y. *Dalton Trans.* **2014**, *43*, 9116. (b) Hu, F.; Zhai, Q.-G.; Li, S.-N.; Jiang, Y.-C.; Hu, M.-C. *CrystEngComm* **2011**, *13*, 414. (c) Chai, W. X.; Wu, L. M.; Li, J. Q.; Chen, L. *Inorg. Chem.* **2007**, *46*, 1042. (d) Chai, W. X.; Wu, L. M.; Li, J. Q.; Chen, L. *Inorg. Chem.* **2007**, *46*, 8698. (e) Fan, L. Q.; Wu, L. M.; Chen, L. *Inorg. Chem.* **2006**, *45*, 3149. (f) Fan, L.-Q.; Huang, Y.-Z.; Wu, L.-M.; Chen, L.; Li, J.-Q.; Ma, E. *J. Solid State Chem.* **2006**, *179*, 2361. (g) Feldmann, C. *Inorg. Chem.* **2001**, *40*, 818.
(8) (a) Tang, C.; Wang, F.; Jia, D.; Jiang, W.; Zhang, Y. *CrystEngComm* **2014**, *16*, 2016. (b) Adonin, S. A.; Sokolov, M. N.; Smolentsev, A. I.; Kozlovaa, S. G.; Fedin, V. P. *Dalton Trans.* **2013**, *42*, 9818. (c) Fang, W.; Tang, C.; Chen, R.; Jia, D.; Jiang, W.; Zhang, Y. *Dalton Trans.* **2013**, *42*, 15150. (d) Burns, M. C.; Tershansy, M. A.; Ellsworth, J. M.; Khalip, Z.; Peterson, L., Jr.; Smith, M. D.; zur Loye, H. C. *Inorg. Chem.* **2006**, *45*, 10437.
(9) CrysAlisPro, Agilent Technologies, Version 1.171.36.28 (release 01-02-2013 CrysAlis171.NET) (compiled Feb 1 2013, 16:14:44).
(10) Clark, R. C.; Reid, J. S. *Acta Crystallogr., Sect. A* **1995**, *A51*, 887.
(11) Altomare, A.; Burla, M. C.; Camalli, M.; Cascarano, G. L.; Giacovazzo, C.; Guagliardi, A.; Grazia, A.; Moliterni, G.; Polidori, G.; Spagna, R. *J. Appl. Crystallogr.* **1999**, *32*, 115.
(12) Betteridge, P. W.; Carruthers, J. R.; Cooper, R. I.; Prout, K.; Watkin, D. J. *J. Appl. Crystallogr.* **2003**, *36*, 1487.
(13) (a) Maudez, W.; Fromm, K. M. *Z. Anorg. Allg. Chem.* **2012**, *638*, 1810. (b) Mishra, S. *Coord. Chem. Rev.* **2008**, *252*, 1996. (c) Fromm, K. M.; Gueneau, E. D.; Bernardinelli, G.; Goesmann, H.; Weber, J.; Mayor-Lopez, M.-J.; Boulet, P.; Chermette, H. *J. Am. Chem. Soc.* **2003**, *125*, 3593. (d) Fromm, K. M.; Maudez, W. *Eur. J. Inorg. Chem.* **2003**, 3440.
(14) Fromm, K. M. *Nat. Chem.* **2013**, *5*, 146.
(15) Matsubara, I.; Paranthaman, M.; Singhal, A.; Vallet, C.; Lee, D. F.; Martin, P. M.; Hunt, R. D.; Feenstra, R.; Yang, C. Y.; Babcock, S. E. *Physica C* **1999**, *319*, 127.
(16) Gschwind, F.; Sereda, O.; Fromm, K. M. *Inorg. Chem.* **2009**, *48*, 10535.
(17) (a) Abbasi, A.; Geranmayeh, S.; Skripkin, M. Y.; Eriksson, L. *Dalton Trans.* **2012**, *41*, 850. (b) Ma, G.; Molla-Abbassi, A.; Kritikos, M.; Ilyukhin, A.; Jalilehvand, F.; Kessler, V.; Skripkin, M.; Sandstrom, M.; Glaser, J.; Naslund, J.; Persson, I. *Inorg. Chem.* **2001**, *40*, 6432. (c) Allen, F. R. *Acta Crystallogr., Sect. B* **2002**, *B58*, 380.
(18) Mishra, S.; Hubert-Pfalzgraf, L. G.; Jeanneau, E. *Polyhedron* **2007**, *26*, 66.
(19) Liao, J.-H.; Latouche, C.; Li, B.; Kahlal, S.; Saillard, J.-Y.; Liu, C. W. *Inorg. Chem.* **2014**, *53*, 2260.
(20) Zhao, Y.; Su, W.; Cao, R.; Hong, M. *Acta Crystallogr. Sect. C* **1999**, *C55*, IUC9900122.
(21) Jalilian, E.; Liao, R.-Z.; Himo, F.; Brismar, H.; Laurell, F.; Lidin, S. *CrystEngComm* **2011**, *13*, 4729.
(22) Ledoux, G.; Guillois, O.; Huisken, F.; Kohn, B.; Porterat, D.; Reynaud, C. *Astron. Astrophys.* **2001**, *377*, 707.
(23) (a) Sun, D.; Yuan, S.; Wang, H.; Lu, H.-F.; Feng, S.-Y.; Sun, D.-F. *Chem. Commun.* **2013**, *49*, 6152. (b) Kitada, N.; Ishida, T. *CrystEngComm* **2014**, *16*, 8035.